

Electronic Supplementary Information

Bifunctional catalysts of Ni nanoparticles coupled MoO₂ nanorods for overall water splitting

Zhiqiang Yao^{1,2}, Chenfeng Wang^{1,2}, Zengyao Wang^{1,2}, Guanglei Liu^{1,3}, Crystal Bowers⁴, Pei Dong⁴, Mingxin Ye^{1}, Jianfeng Shen^{1*}*

¹Institute of Special Materials and Technology, Fudan University, Shanghai 200433, China

²Department of Chemistry, Fudan University, Shanghai, 200433, P. R. China

³Department of Materials Science, Fudan University, Shanghai, 200433, P. R. China

⁴Department of Mechanical Engineering, George Mason University, VA 22030, USA

*Correspondence to: mxye@fudan.edu.cn, jfshen@fudan.edu.cn

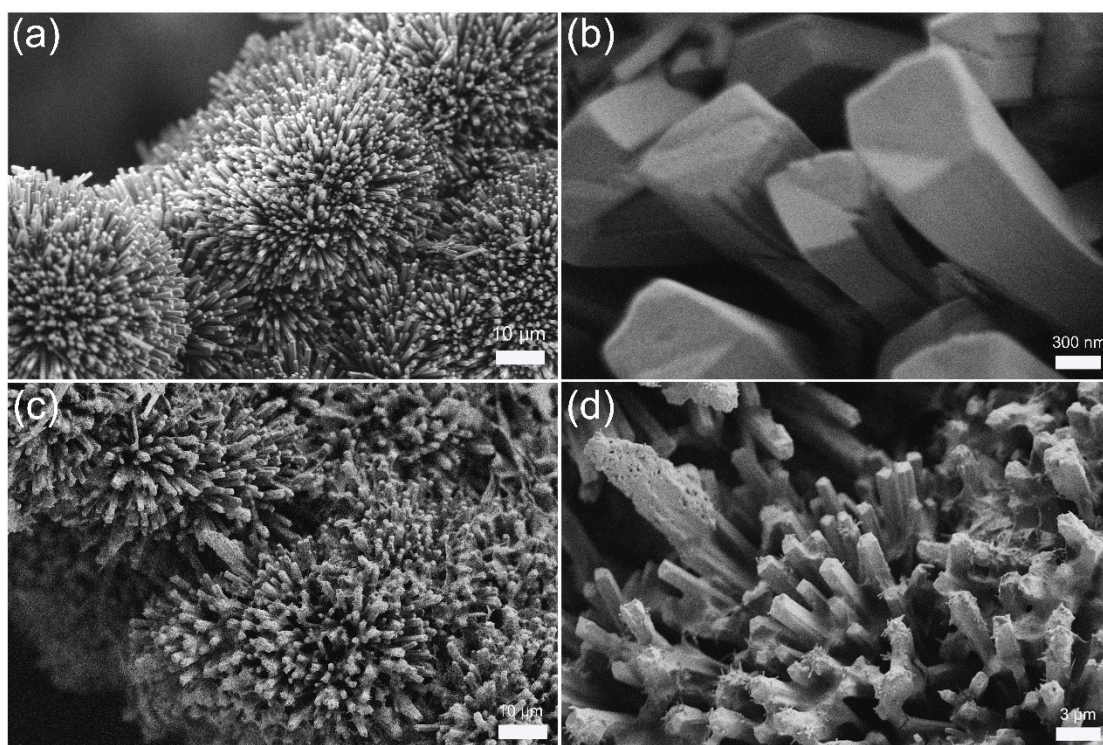


Fig. S1. SEM images of (a, b) NiMoO₄·xH₂O and (c, d) NMO-ZIF.

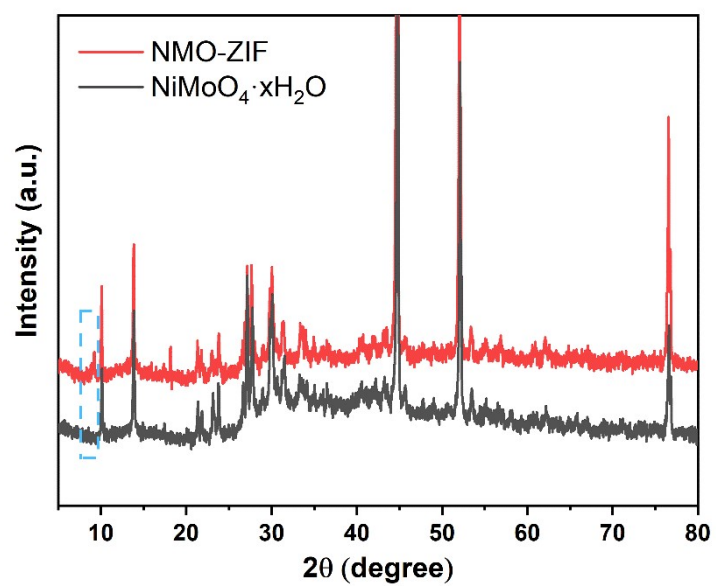


Fig. S2. XRD images of NiMoO₄·xH₂O and NMO-ZIF.

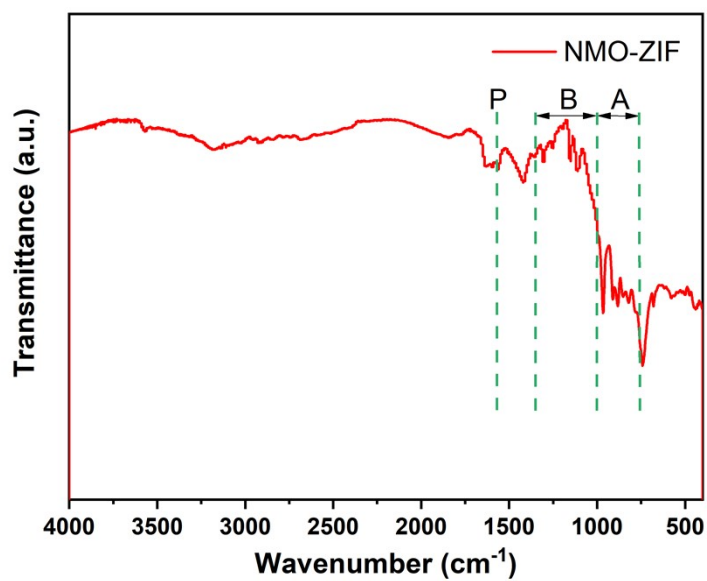


Fig. S3. FTIR spectrum of NMO-ZIF.

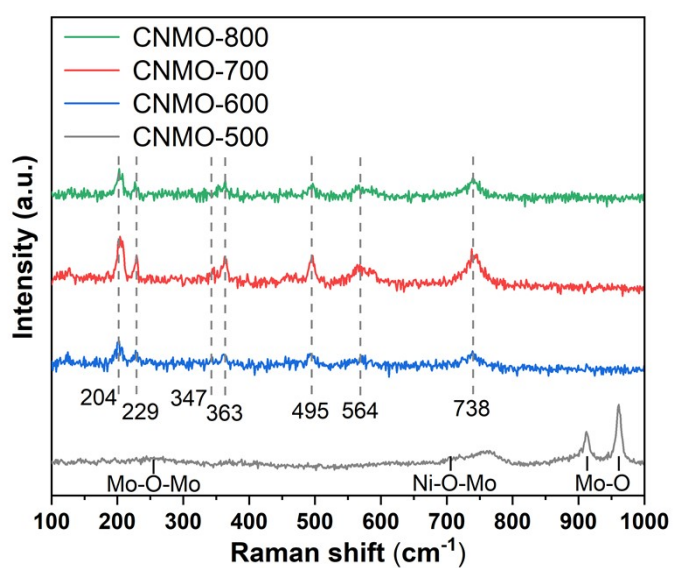


Fig. S4. Raman spectra of CNMOs at different calcination temperatures.

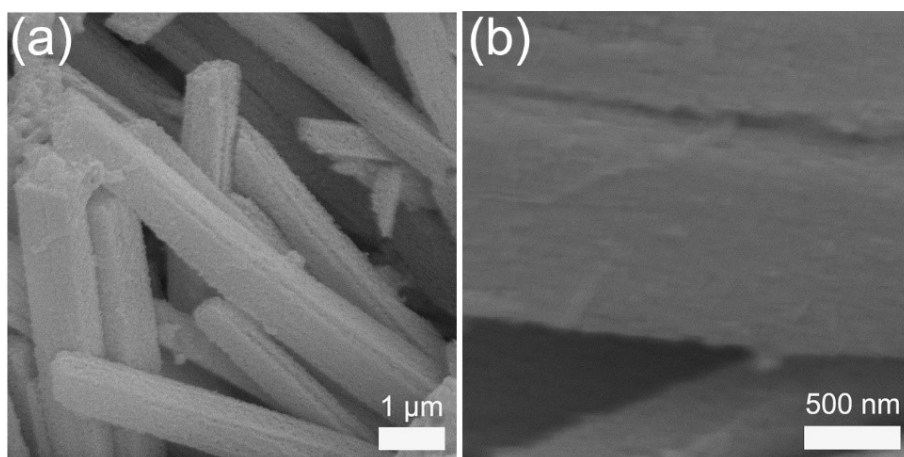


Fig. S5. SEM images of CNMO-700 after acid etching.

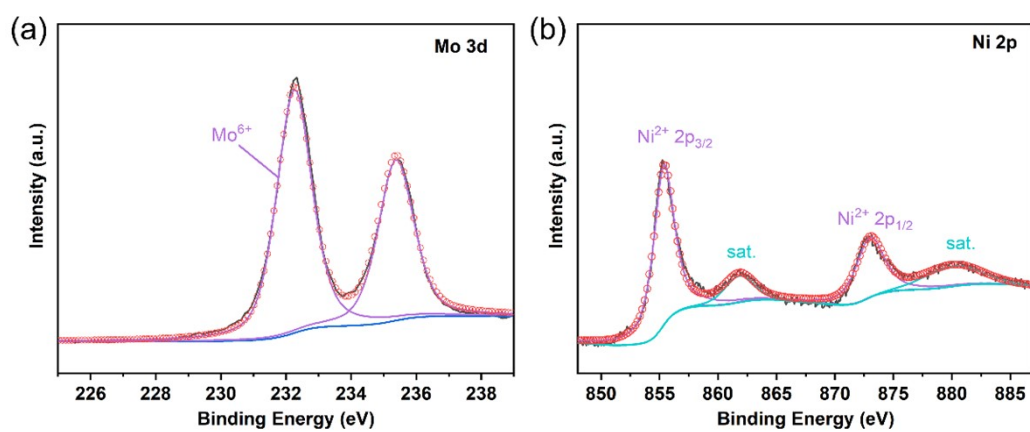


Fig. S6. XPS spectra of CNMO-500. (a) Mo 3d, (b) Ni 2p.

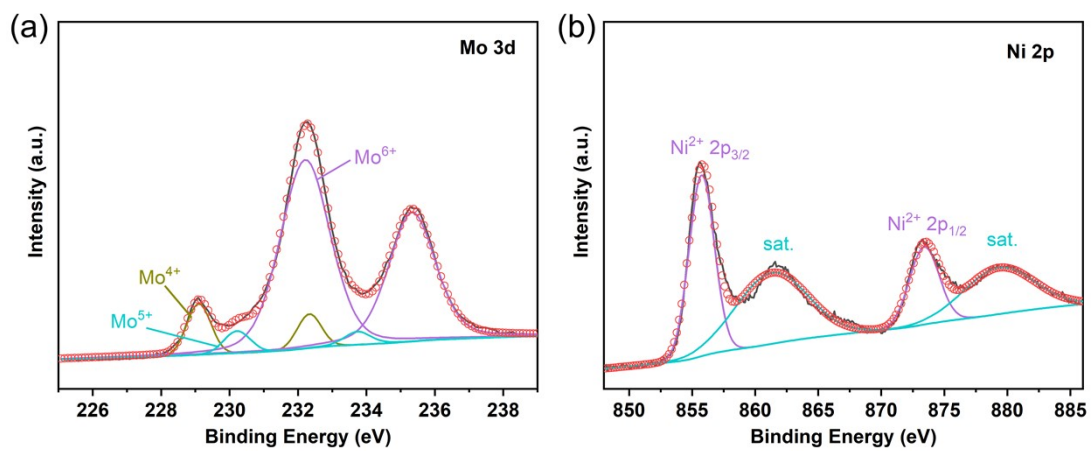


Fig. S7. XPS spectra of MoO₂. (a) Mo 3d, (b) Ni 2p.

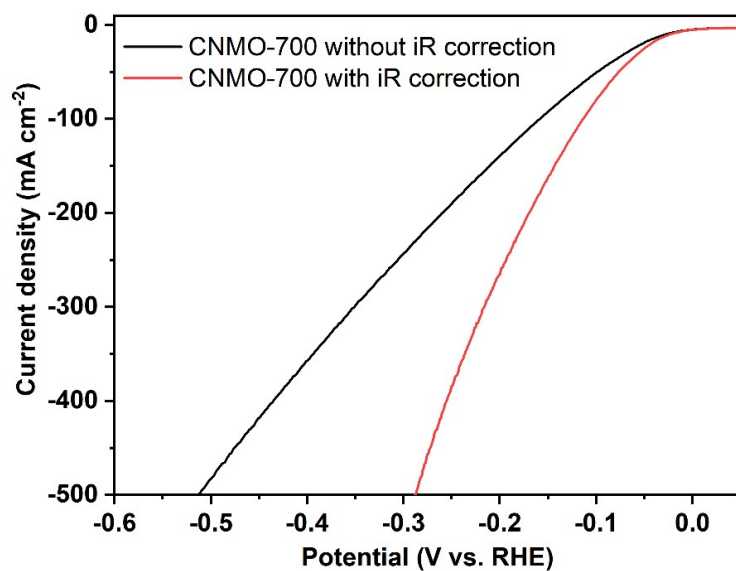


Fig. S8. LSV curves of CNMO-700 with/without iR correction for HER.

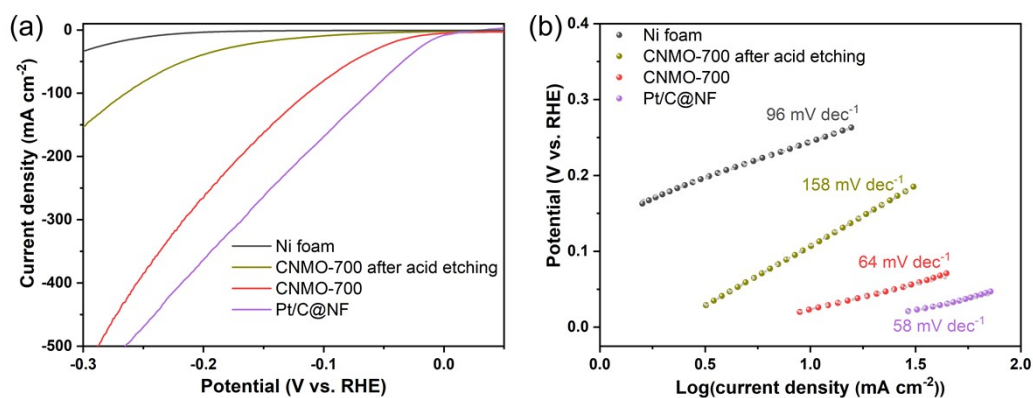


Fig. S9. (a) LSV curves and (b) Tafel slopes of Ni foam, CNMO-700 after acid etching, Pt/C and CNMO-700 for HER.

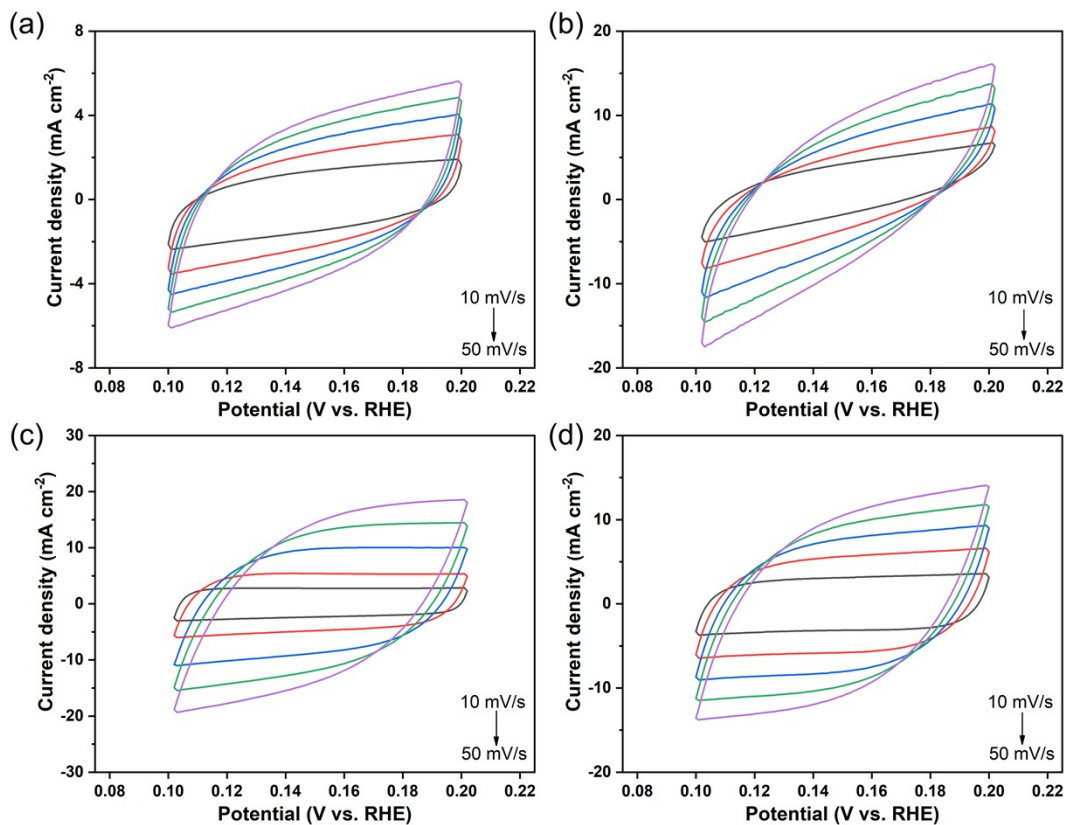


Fig. S10. Typical cyclic voltammograms of CNMO-500, 600, 700, 800 at scan rates ranging from 10 to 50 mV s⁻¹, the scanning potential range is from 0.10 V to 0.20 V.

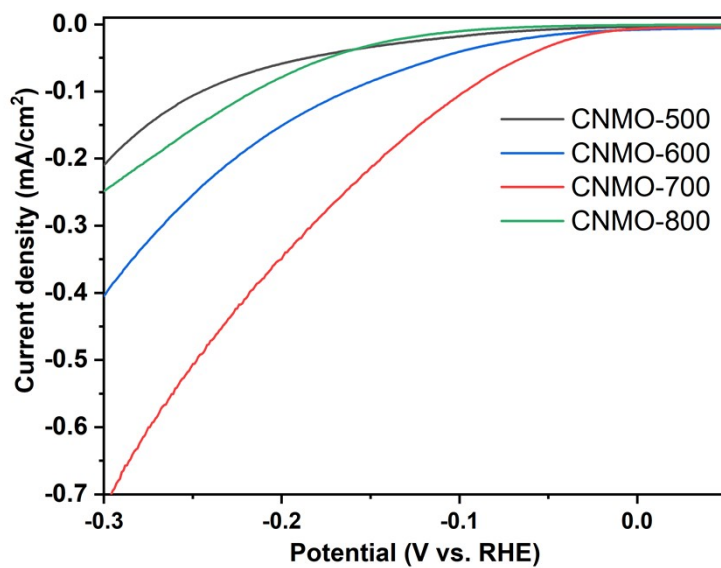


Fig. S11. HER activity (current density) of the samples normalized by their ECSAs.

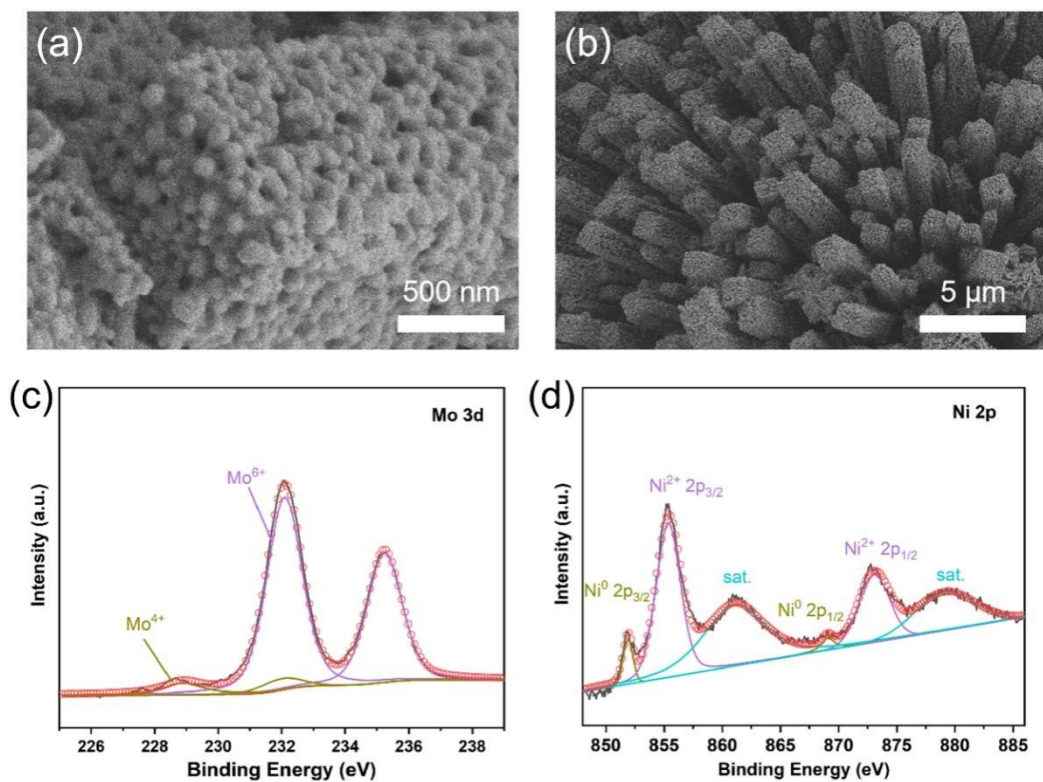


Fig. S12. (a, b) SEM images and (c, d) XPS spectra of CNMO-700 after hydrogen evolution stability test.

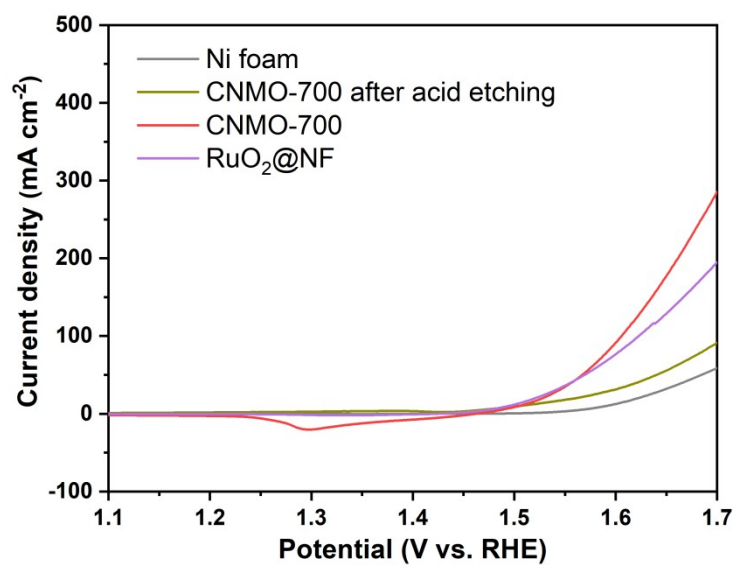


Fig. S13. LSV of Ni foam, CNMO-700 after acid etching, CNMO-700, RuO₂ for OER.

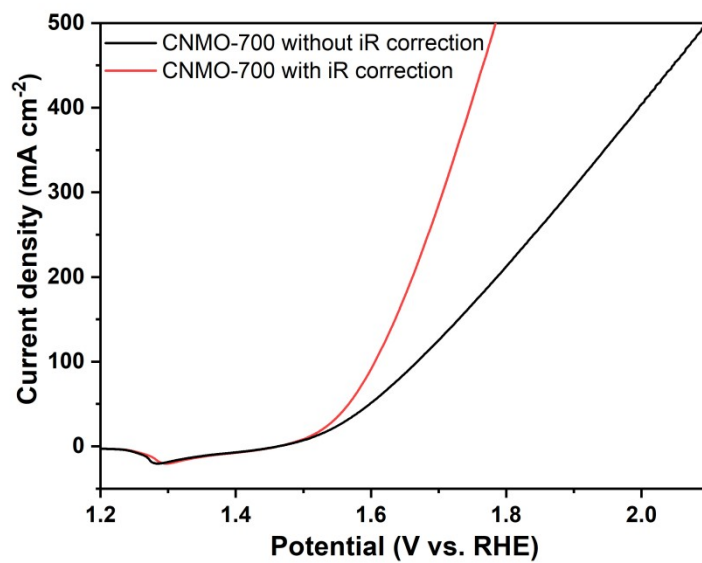


Fig. S14. LSV curves of CNMO-700 with and without iR correction for OER.

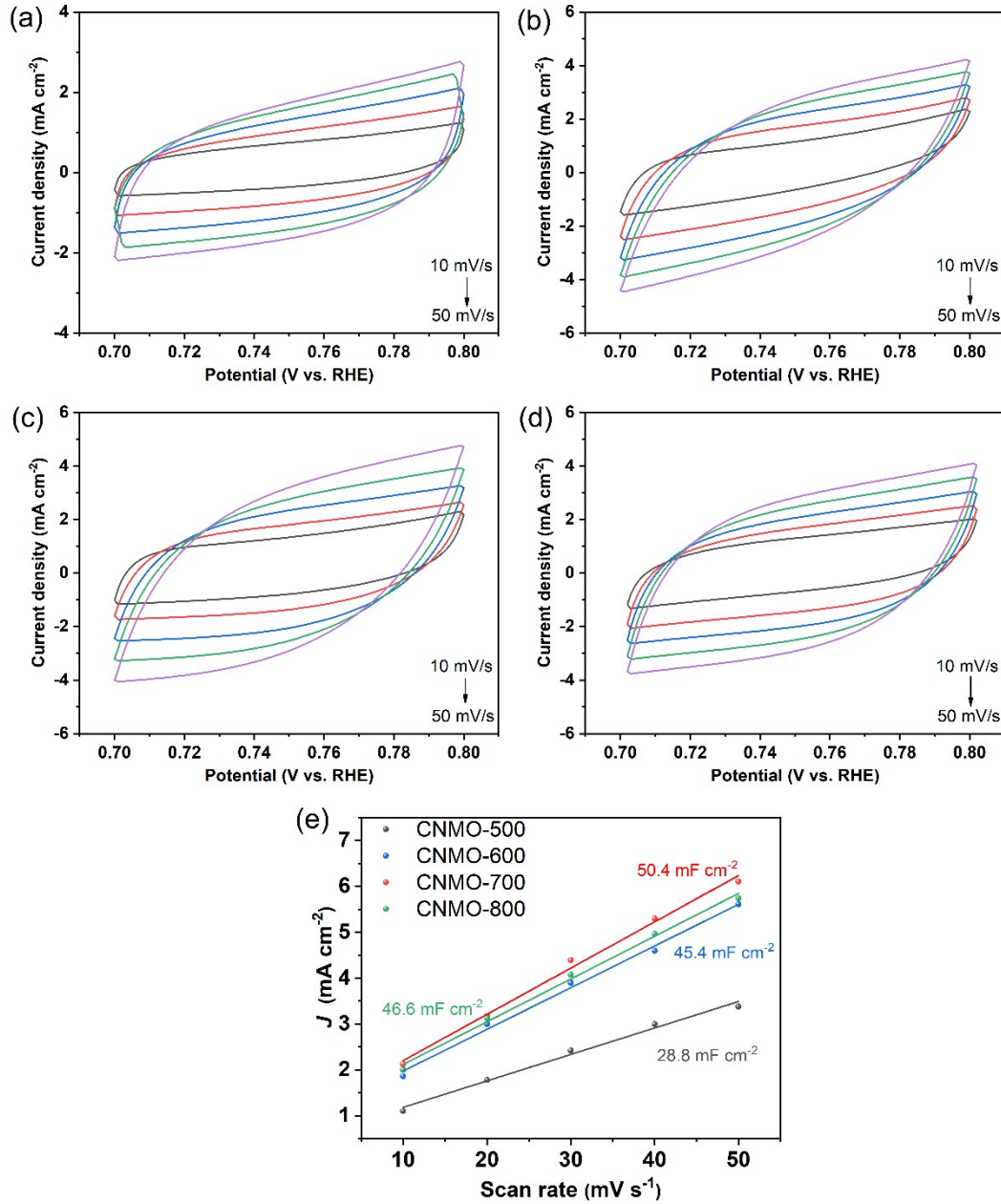


Fig. S15. (a-d) Typical cyclic voltammograms (CV) of CNMO-500, 600, 700, 800 at scan rates ranging from 10 to 50 mV s⁻¹, the scanning potential range is from 0.7 V to 0.8 V. (e) ECSA estimated by C_{dl} values.

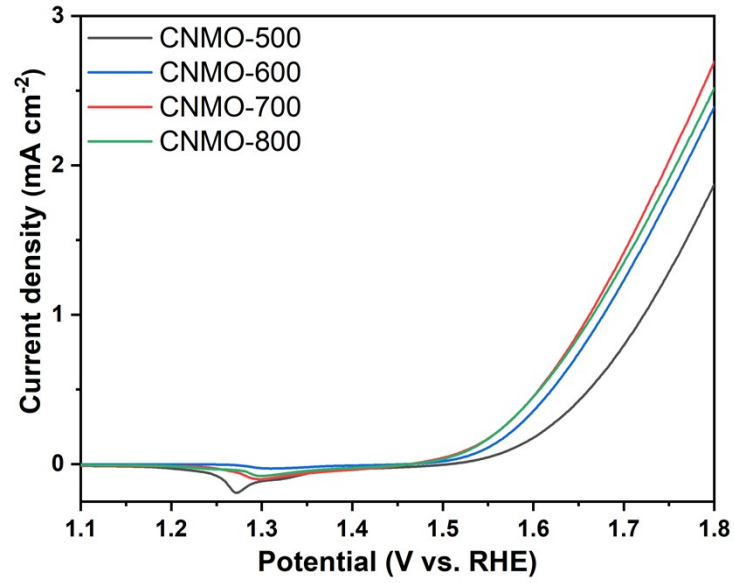


Fig. S16. OER activity (current density) of the samples normalized by their ECSAs.

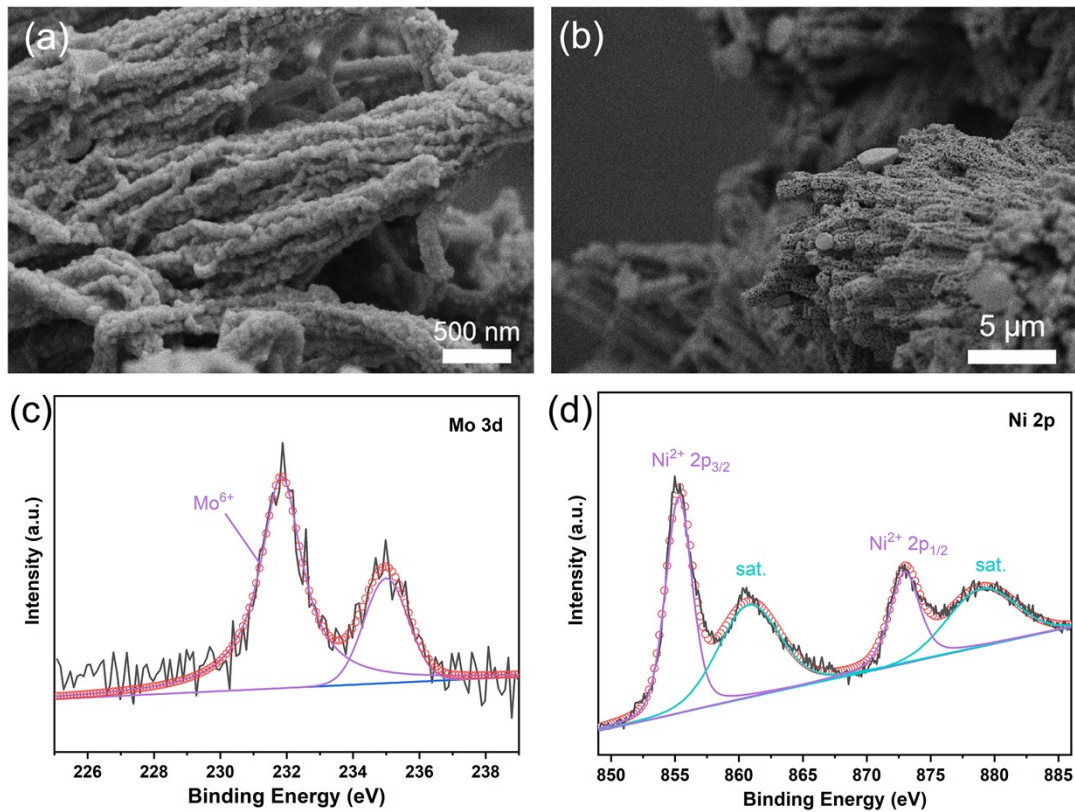


Fig. S17. (a, b) SEM images and (c, d) XPS spectra of CNMO-700 after OER stability test.

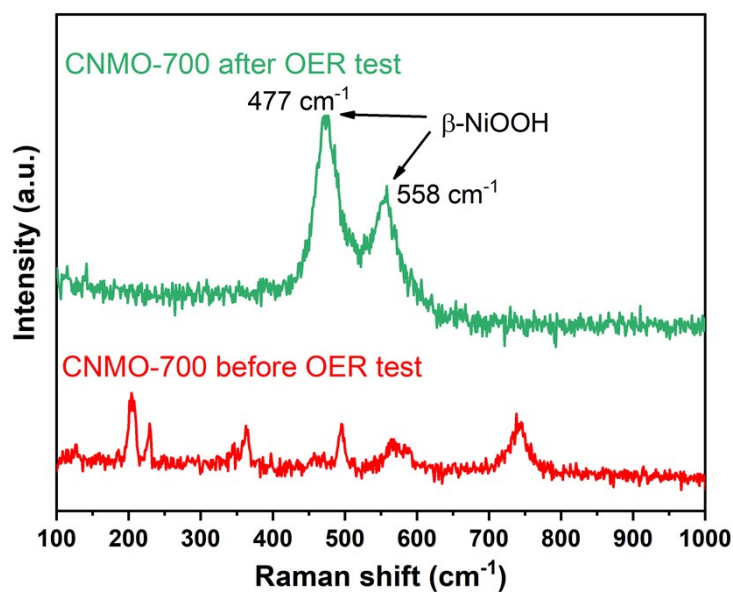


Fig. S18. Raman spectrum of the CNMO-700 before and after OER test.

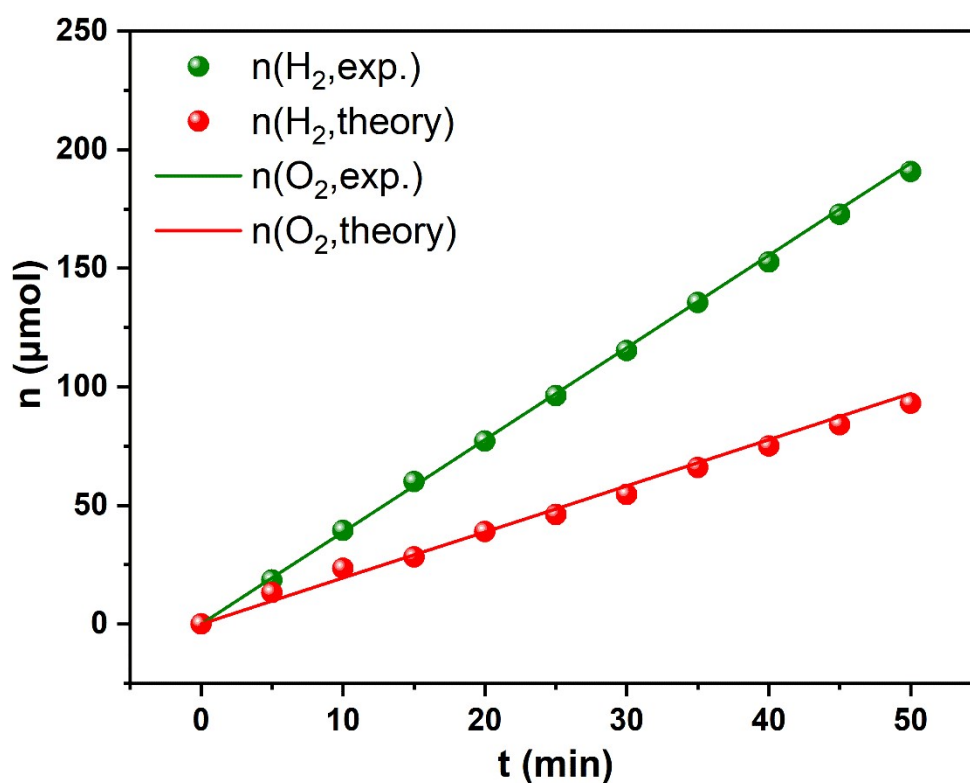


Fig. S19. The amount of gas theoretically calculated and experimentally measured versus time for overall water splitting at the current density of 50 mA cm^{-2} .

Table S1. Comparison of HER, OER and overall water splitting activity of Ni-MoO₂ with other TMO-based bifunctional electrocatalysts in 1 M KOH.

Materials	HER		OER		Overall	Ref.
	η_{10}	Tafel slope	η_{10}	Tafel slope	E_{10}	
	(mV)	(mV dec ⁻¹)	(mV)	(mV dec ⁻¹)	(V)	
Ni-MoO ₂	24	64	275	81	1.55	This work
NiO-Ni ₃ S ₂	71	70	290	75	1.57	[1]
CF@Ni@NiO	153	84	300	60	1.65	[2]
NiFeP-MoO ₂	56	81	149	29	1.41	[3]
Ni ₂ P/MoO ₂ @MoS ₂	159	77	280	85	1.72	[4]
N-NiMoO ₄ /NiS ₂	99	74	283	44	1.60	[5]
NiMoO _{4-x} /MoO ₂	41	31	233	69	1.56	[6]
NiCo ₂ O ₄	110	50	~280	53	1.65	[7]
Co-Fe NPs	220	73	340	51	1.92	[8]
Ni _x Co _{1-x} MoO ₄ @CoMoO ₄	61	63	180	43	1.46	[9]
P-Co ₃ O ₄	120	52	280	51.6	1.69	[10]
ceria/Ni-TMO	93	69	220	38	1.58	[11]
Co@Co ₃ O ₄ /FeNS-RGO	130	108	287	69	1.65	[12]
NF/H-CoMoO ₄	42	91	295	/	1.56	[13]
CoNiMo-O	60	73	280	65	1.59	[14]

References.

1. L. Peng, J. Shen, X. Zheng, R. Xiang, M. Deng, Z. Mao, Z. Feng, L. Zhang, L. Li and Z. Wei, *Journal of Catalysis*, 2019, **369**, 345-351.
2. Z. Zhang, S. Liu, F. Xiao and S. Wang, *ACS Sustainable Chemistry & Engineering*, 2016, **5**, 529-536.
3. X. F. Wu, J. W. Li, Y. Li and Z. H. Wen, *Chemical Engineering Journal*, 2021, **409**.
4. Y. Wang, T. Williams, T. Gengenbach, B. Kong, D. Y. Zhao, H. T. Wang and C. Selomulya, *Nanoscale*, 2017, **9**, 17349-17356.
5. J. G. Li, K. Xie, H. Sun, Z. Li, X. Ao, Z. Chen, K. K. Ostrikov, C. Wang and W. Zhang, *ACS Appl Mater Interfaces*, 2019, **11**, 36649-36657.
6. Z. Zhang, X. Ma and J. Tang, *Journal of Materials Chemistry A*, 2018, **6**, 12361-12369.
7. X. Gao, H. Zhang, Q. Li, X. Yu, Z. Hong, X. Zhang, C. Liang and Z. Lin, *Angew Chem Int Ed Engl*, 2016, **55**, 6290-6294.
8. W. Adamson, X. Bo, Y. Li, B. H. R. Suryanto, X. Chen and C. Zhao, *Catalysis Today*, 2020, **351**, 44-49.
9. Z. K. Li, M. Y. Zheng, X. Zhao, J. Yang and W. L. Fan, *Nanoscale*, 2019, **11**, 22820-22831.
10. Z. Xiao, Y. Wang, Y.-C. Huang, Z. Wei, C.-L. Dong, J. Ma, S. Shen, Y. Li and S. Wang, *Energy & Environmental Science*, 2017, **10**, 2563-2569.
11. X. Long, H. Lin, D. Zhou, Y. An and S. Yang, *ACS Energy Letters*, 2018, **3**, 290-296.
12. J. Zhu, W. Tu, Z. Bai, H. Pan, P. Ji, H. Zhang, Z. Deng and H. Zhang, *Electrochimica Acta*, 2019, **323**.
13. K. Chi, X. Tian, Q. Wang, Z. Zhang, X. Zhang, Y. Zhang, F. Jing, Q. Lv, W. Yao, F. Xiao and S. Wang, *Journal of Catalysis*, 2020, **381**, 44-52.
14. B. Ren, D. Li, Q. Jin, H. Cui and C. Wang, *ChemElectroChem*, 2019, **6**, 413-420.